

Magnetic field screening and mirroring in graphene

Mikito Koshino, Yasunori Arimura, and Tsuneya Ando

Department of Physics, Tokyo Institute of Technology, Tokyo 152-8551, Japan

(dated: April 2, 2024)

The orbital magnetism in spatially varying magnetic fields is studied in monolayer graphene within the effective mass approximation. We find that, unlike the conventional two-dimensional electron system, graphene with small Fermi wave number k_F works as a magnetic shield where the field produced by a magnetic object placed above graphene is always screened by a constant factor on the other side of graphene. The object is repelled by a diamagnetic force from the graphene, as if there exists its mirror image with a reduced amplitude on the other side of graphene. The magnitude of the force is much greater than that of conventional two-dimensional system. The effect disappears with the increase of k_F .

Graphene, an atomic sheet of graphite, has a peculiar electronic structure analogous to a relativistic particle, and its unique properties have been of great interest. In graphene the conduction and valence bands stick together with a linear dispersion. The low-energy physics is successfully described by the effective-mass Hamiltonian analogous to the massless Dirac Fermion, [1, 2, 3, 4] and its unique transport properties were studied. [4, 5, 6, 7, 8] Since its experimental fabrication, [9, 10, 11] the graphene and related materials have attracted much attention and have been extensively investigated in experiments and theories.

The electronic property of graphene in a magnetic field was first investigated in theories as a simple model of the bulk graphite. [12] There it was shown that, in a uniform magnetic field, graphene exhibits a huge diamagnetic susceptibility due to the orbital motion of electrons, which is quite different from the conventional Landau diamagnetism. The orbital magnetism was also studied for related materials such as the bulk graphite, [13, 14] graphite intercalation compounds, [15, 16, 17] carbon nanotube, [18, 19] disordered graphene, [20, 21, 22] few-layered graphenes, [23, 24, 25] and nodal Fermions [26]. Quite recently, the graphene in a spatially modulated magnetic field was studied in the context of the electron confinement using magnetic barrier. [27, 28, 29] The diamagnetic susceptibility was experimentally observed for quasi-two-dimensional graphite, which is a random stack of graphene sheets. [30]

In this paper, we study the orbital diamagnetism in non-uniform magnetic fields in monolayer graphene. Using the effective mass approximation and the perturbation theory, we calculate the electric current induced by an external magnetic field with wavenumber q , to obtain susceptibility $\chi(q)$ for general Fermi energies. We apply the result to arbitrary geometries where a certain magnetic object is located above graphene, and estimate the response current induced on graphene, as well as the diamagnetic repulsive force which works between graphene and the magnetic object. We find that graphene has a peculiar property of magnetic mirroring, where the counter field induced by the response current mimics a mirror

image of the original object.

We start with the general formulation of the electric response to the spatially-varying magnetic field in a two-dimensional (2D) system. We assume a uniform 2D system on the xy plane, and apply a magnetic field perpendicular to the layer $B(r) = [r \cdot A(r)]_z$ with vector potential $A(r)$. Here $r = (x; y)$ denotes 2D position on the graphene while we later use $\mathbf{r} = (x; y; z)$ to specify the point in three-dimensional (3D) space. We define $\mathbf{j}(r) = (j_x; j_y)$ as the 2D electric current density induced by the magnetic field. Within the linear response, the Fourier-transforms of $\mathbf{j}(r)$ and $A(r)$ are related by

$$\mathbf{j}(q) = \int d\mathbf{r} K(q) A(q); \quad (1)$$

with response function K . The gauge invariance for A requires $\int d\mathbf{r} K(q) q = 0$. The continuous equation in the static system, $\nabla \cdot \mathbf{j}(r) = 0$, imposes another constraint $q \cdot K(q) = 0$. To meet both requirements, tensor K needs to be in the form,

$$K(q) = K(q) \frac{q_i q_j}{q^2} : \quad (2)$$

On the other hand, because $\nabla \cdot \mathbf{j}(r) = 0$, we can express $\mathbf{j}(r)$ as $j_x = c \partial_m \phi_y$, $j_y = -c \partial_m \phi_x$; with $m(r)$ being the local magnetic moment perpendicular to the layer, and the light velocity c . In the linear response, its Fourier transform is written as

$$m(q) = \chi(q) B(q); \quad (3)$$

with the magnetic susceptibility $\chi(q)$. Equations (1) and (3) are complementary, and both response functions $\chi(q)$ and $K(q)$ are related by

$$\chi(q) = \frac{1}{c q^2} K(q); \quad (4)$$

Graphene is composed of a honeycomb network of carbon atoms, where a unit cell contains a pair of sublattices, denoted by A and B . The conduction and valence bands touch at the Brillouin zone corners called K and

K^0 points, where the Fermi energy lies. The effective-mass Hamiltonian near a K point in the absence of a magnetic field is given by [1, 2, 3, 4]

$$H_0 = \sim v \begin{pmatrix} 0 & \hat{k}_x & \hat{k}_y \\ \hat{k}_x + i\hat{k}_y & 0 & 0 \\ 0 & 0 & 0 \end{pmatrix} = \sim v \hat{k} \quad ; \quad (5)$$

where v is the constant velocity, $\hat{k} = (\hat{k}_x; \hat{k}_y) = i\sigma \cdot \mathbf{k}$, and $\sigma = (\sigma_x; \sigma_y)$ are the Pauli matrices. The Hamiltonian (5) operates on a two-component wave function $(\psi_A; \psi_B)$ which represents the envelope functions at A and B sites. The eigenstates are labeled by $(s; \mathbf{k})$ with $s = +1$ and -1 being the conduction and valence bands, respectively, and \mathbf{k} being the wavevector. The eigenenergy is given by $\epsilon_{s\mathbf{k}} = s\sim v k$, and the corresponding wavefunction is $\psi_{s\mathbf{k}}(\mathbf{r}) = e^{i\mathbf{k} \cdot \mathbf{r}} F_{s\mathbf{k}} = \frac{1}{\sqrt{2}} \begin{pmatrix} e^{i\mathbf{k} \cdot \mathbf{r}} \\ s \end{pmatrix}$, where \mathbf{k} and \mathbf{r} are defined by $(k_x; k_y) = k(\cos \theta; \sin \theta)$ and S is the system area.

In a magnetic field $B(\mathbf{r}) = [B_0 \cos q x]$, the Hamiltonian becomes $H = H_0 + H_1$ with $H_1 = (e\sim v c) A(\mathbf{r})$. The local current density at \mathbf{r}_0 is calculated as the expectation value of current-density operator $\hat{j}(\mathbf{r}_0) = e\sim v (\mathbf{r} \times \mathbf{p})$ over the occupied states. In the first order perturbation in H_1 , we have

$$K(q) = \frac{g_v g_s e^2 v^2}{c} \frac{1}{S} \sum_{s s^0 \mathbf{k}} \frac{f(\epsilon_{s\mathbf{k}}) - f(\epsilon_{s^0 \mathbf{k} + \mathbf{q}})}{\epsilon_{s\mathbf{k}} - \epsilon_{s^0 \mathbf{k} + \mathbf{q}}} \quad (6)$$

where $g_v = g_s = 2$ are the valley (K, K^0) and spin degeneracy, respectively, and $f(\epsilon) = [1 + \exp(\epsilon / (k_B T))]^{-1}$ with $T = 1/(k_B T)$ is the Fermi distribution function.

At the zero temperature, we can explicitly calculate this to obtain

$$K(q; \mu_F) = \frac{g_v g_s e^2 v^2}{16\sim c^2} \frac{1}{q} \left(1 - \frac{2k_F}{q} \right) \quad ; \quad (7)$$

where $k_F = \mu_F / (\sim v)$ is the Fermi wave number and $\theta(x)$ is defined by $\theta(x) = 1$ ($x > 0$) and 0 ($x < 0$). Significantly, $K(q)$ vanishes in range $q < 2k_F$, i.e., no electric current is induced when the external field is smooth enough compared to the Fermi wavelength. At $\mu_F = 0$, particularly, we have

$$K(q; \mu_F = 0) = \frac{g_v g_s e^2 v^2}{16\sim c^2} \frac{1}{q} \quad (8)$$

The susceptibility of the carbon nanotube to a uniform field perpendicular to the axis has the equivalent expression of Eq. (8) where q is replaced by $2\pi/L$ with tube circumference L . [18, 19] Figure 1 (a) shows a plot of $K(q)$ of Eq. (7). The susceptibility suddenly starts from zero at $q = 2k_F$, and rapidly approaches the universal curve

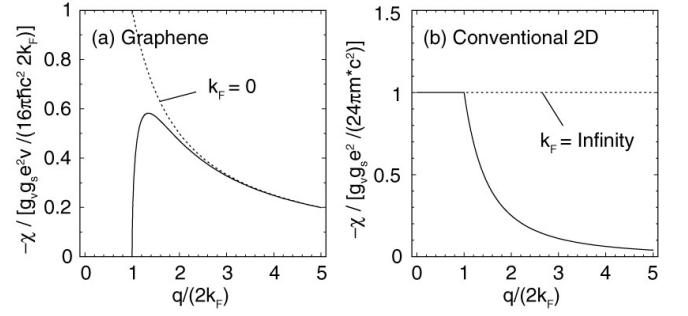


FIG. 1: Magnetic susceptibility $K(q)$ in (a) graphene and (b) conventional 2D system.

(8). As a function of μ_F at fixed q , it is nonzero only in a finite region satisfying $\mu_F < \sim v q/2$, and its integral over μ_F becomes constant $g_v g_s e^2 v^2 / (6\sim c^2)$. Thus, in the limit of $q \rightarrow 0$ it goes to

$$K(q = 0; \mu_F) = \frac{g_v g_s e^2 v^2}{6\sim c^2} (\mu_F) \quad (9)$$

This agrees with the susceptibility against uniform magnetic field. [12, 23]

Let us consider an undoped graphene ($\mu_F = 0$) under a sinusoidal field $B(\mathbf{r}) = B_0 \cos q x$. With the susceptibility of Eq. (7), the response current is calculated as $j(\mathbf{r}) = [g_v g_s e^2 v B_0 / (16\sim c)] e_y \sin q x$. The current induces a counter magnetic field which reduces the original field. The z component of the induced field on graphene becomes

$$B_{ind}(\mathbf{r}) = -g B(\mathbf{r}); \quad g = \frac{2 g_v g_s e^2 v}{16\sim c^2} \quad (10)$$

Because the ratio is independent of q , Eq. (10) is actually valid for any external field $B(\mathbf{r})$, i.e., the magnetic field on the graphene is always reduced by the same factor $1 - g$. This property holds whenever $K(q)$ is proportional to $1/q$. With the typical value $v \approx 10^6$ m/s, g is estimated as 4×10^5 , showing that the counter field is much smaller than the original.

The argument of the magnetic field screening can be extended in the three dimensional field distribution. Let us suppose a situation when a certain magnetic object (permanent magnet or electric current) is located above the undoped graphene ($z > 0$), which produces an external magnetic field $B(\mathbf{r})$ in 3D space $\mathbf{r} = (x; y; z)$. Then, the followings can easily be concluded: (i) On the other side of the graphene ($z < 0$), the induced field becomes $-g B(\mathbf{r})$, i.e., the external field is screened by the factor $1 - g$. (ii) On the same side ($z > 0$), the induced field is given by $-g R_z [B(x; y; z)]$, where R_z is the vector inversion with respect to $z = 0$. Namely, this is equivalent to a field of the mirror image of the original object reflected with respect to $z = 0$, and reduced by g .

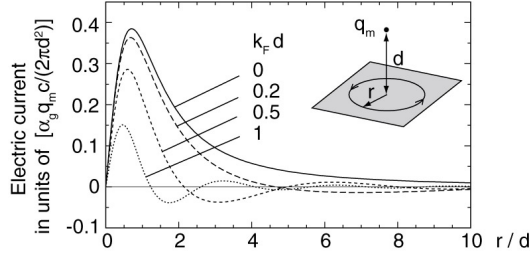


FIG. 2: Electric current $j(r)$ on graphene induced by a magnetic charge q_m at $z = d$.

For examples, we can calculate the diamagnetic electric current and the induced field in several specific geometries. We first take a situation where a magnetic charge (monopole) q_m is located at the point $\mathbf{r}_0 = (0; 0; d)$; ($d > 0$) above the graphene plane $z = 0$. The magnetic field perpendicular to the layer on the graphene is given by $B(r) = q_m d / (r^2 + d^2)^{3/2}$ with $r = (x^2 + y^2)^{1/2}$. For $\mu_F = 0$, induced m is calculated as $m(r) = (-g q_m / 2) (r^2 + d^2)^{-1/2}$, and the corresponding current density is given by $j(r) = -c(\partial m / \partial r) e$ with e being an azimuthal unit vector on the xy plane. We note that the integral of $m(r)$ over the plane is infinite, showing that it never looks like a single magnetic dipole even if observed from far away. Indeed, the counter field in region $z > 0$ induced by j is the monopole field given by $g q_m$ located at \mathbf{r}_0 , as expected from the general argument above. The monopole is thus repelled away from the graphene with a force of $g^2 q_m^2 = (2d)^2$.

For doped graphenes $\mu_F \neq 0$, we numerically calculate the response current. Figure 2 shows $j(r)$ for several values of k_F . We observe the Friedel-type oscillation with wavenumber $2k_F$. The overall amplitude exponentially decays in region $k_F \ll 1/d$ because the magnetic field distribution on graphene has a typical length scale of the order of d , while $\chi(q)$ vanishes in the long-wavelength region such as $q < 2k_F$.

As another example, we consider line current I parallel to the graphene, which flows along the $+y$ direction, passing through the point $(0; 0; d)$ ($d > 0$) above graphene. The z component of the magnetic field on graphene is given by $B(r) = 2_0 I x / [c(x^2 + d^2)]$; For $\mu_F = 0$, the induced current density becomes $j(r) = (g I d / c) (x^2 + d^2)^{-1} e_y$: The integral of j_y in x exactly becomes $g I$, i.e., the external electric current induces an opposite current on graphene with the amplitude reduced by g . The magnetic field induced by j in the upper half space ($z > 0$) becomes equivalent to a field made by current $g I$ flowing at $z = d$, so that the original current is repelled by a force $g^2 I^2 = (c^2 d)$ per unit length. When $\mu_F \neq 0$, the response current damps for $k_F d \ll 1$, similarly to the case of a magnetic monopole.

To estimate the diamagnetic force in a possible real-

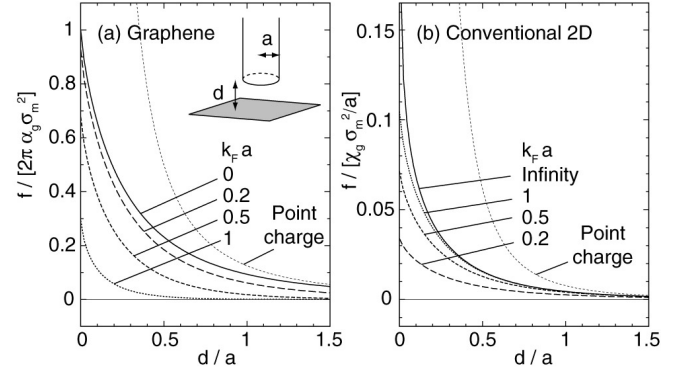


FIG. 3: Diamagnetic force per unit area of a semi-infinite magnet cylinder with radius a as a function of the distance d from the tip to (a) graphene and (b) conventional 2D system.

istic situation, we consider a case where a semi-infinite magnet cylinder with radius a , having a flat end with surface magnetic charge density σ_m , is placed vertically above graphene. In real experiments, a may range from nanoscale (~ 10 nm) up to macroscopic length scale. Figure 3 (a) shows the repulsive force per unit area on the magnet surface, as a function of the distance d from the graphene with several values of k_F . The geometry is illustrated in the inset. For $k_F = 0$, the force is equivalent to that made by its mirror charge $g \sigma_m$ under graphene. When $d \ll a$, it approaches the dotted curve given by $f \propto 1/d^2$, the force when the surface charge is replaced with a point charge $q_m = a^2 \sigma_m$. As d goes down to the order of a , it deviates from $1/d^2$ and reaches $2 g^2 \sigma_m^2$ at $d = 0$, which is exactly the force between a sheet with the magnetic charge density σ_m and another sheet with $g \sigma_m$, with an infinite small gap. For σ_m which amounts to the surface flux of 1 T (e.g., neodymium magnet), [31] the force is estimated as 0.16 gram force/cm², which is surprisingly large as a force generated by a film only one atom thick.

When k_F shifts from zero, the force becomes smaller. The tail is truncated at $d \sim 1/k_F$, i.e., the repulsive force is lost when the distance exceeds the order of the Fermi wavelength. This is due to the absence of $\chi(q)$ for long wavelength $q < 2k_F$ argued above. Similarly, the value at $d = 0$ also decays when k_F exceeds the order of $1/a$, because at $d = 0$ the spatial distribution of B on the graphene has a typical length scale a .

The graphene diamagnetism is in striking contrast to that of the conventional 2D system. If we apply the similar argument to Hamiltonian $H = (p + eA/c)^2 / (2m)$, the nonlocal susceptibility corresponding to Eq. (7) yields

$$\chi(q; \mu_F) = \frac{g_v g_s e^2}{24 m c^2} \left[1 - \frac{4 k_F^2}{q^2} \right]^{3/2} \chi(2k_F) \quad (11)$$

with $\mu_F = \hbar^2 k_F^2 / (2m)$. The plot is shown in Fig.

1 (b). When $q < 2k_F$, this is constant at $\mu_0 g_s e^2 = (24 \text{ m}^{-2})$, which agrees with the usual Landau diamagnetism. In the region satisfying $q > 2k_F$, decays approximately in proportion to $1/q^2$. In highly-doped systems such that k_F is much larger than the typical length scale of external field $B(r)$, the induced magnetization just becomes $m(r) = \mu_0 B(r)$. For the case of a magnetic charge at $z = d$, we have $m(r) / d = (r^2 + d^2)^{-3/2}$, and the integral of $m(r)$ over the plane is now finite. The induced magnetic field at the distance $R = d$ is thus dipole-type decaying in proportion to $1/R^3$, in contrast to the monopole-type field $1/R^2$ in graphene.

Figure 3 (b) shows the force per unit area of the cylindrical magnet with radius a placed above the conventional 2D system. At large distance $d \gg a$, it rapidly decreases as $1/d^3$ like in the case of a point magnetic charge. The peak value at $d = 0$ has a typical amplitude $\mu_0^2 m^2 = a^2$ with a factor $\log k_F a$. Apart from the factor, the ratio of the force at $d = 0$ of the undoped graphene to that of the conventional 2D metal is given by $2 g a = 0$, which is roughly the ratio of the values of q at $q = 1/a$. When the effective mass of GaAs $m^* = 0.067 m_0$ is applied to μ_0 , the ratio becomes $a = (0.01 \text{ nm})$. Thus, in a realistic dimension, the diamagnetic force of the graphene is incomparably larger than that of the conventional 2D system. Note that, in doped graphene, the diamagnetism disappears when a becomes larger than k_F^{-1} . It should be noted that q of graphene does not approach that of conventional 2D even in the high k_F limit, because of difference between linear and quadratic dispersions.

The singular diamagnetism of graphene is influenced by temperature. At zero doping, we expect that q deviates from $1/q$ in $\sim v q$. $k_B T$, and the divergence at $q = 0$ is rounded to a finite value $1/(k_B T)$. In other words, the temperature affects diamagnetism when the typical length scale exceeds $2 \sim v/k_B T$, which is 50 m at $T = 1 \text{ K}$. We expect that the disorder potential gives a roughly similar effects to temperature, where the energy scale of level broadening works as finite $k_B T$. [21, 22]

The magnetism is also contributed by electron spins. The spin susceptibility $\chi^{\text{spin}}(q)$ is given by the usual density-density response function. [32, 33] At $\mu_F = 0$, this becomes $g_v^2 q^2 = (16 \sim v)$ with the Bohr magneton μ_B , in contrast to the orbital susceptibility $\chi^{\text{orb}} / 1 = q$ in Eq. (8). The ratio $\chi^{\text{spin}} = \chi^{\text{orb}} (q = 0.04 \text{ nm}^{-1})$, is quite small in realistic length scales. We also mention that strongly disordered graphite [34] and graphene [35] exhibit ferromagnetism due to spin ordering at lattice defects. [25]

The diamagnetism can be enhanced by stacking graphene films. If we have randomly stacked graphenes where the interlayer hopping is neglected, [30, 36, 37] the magnetic field would decay exponentially $1/(1 - g)^N$ with the layer number N . We would have an almost perfect magnetic shield when $N g$ exceeds 1, which amounts to the thickness of 10 m with the graphite interlayer spacing 0.334 nm assumed. We also expect that a strong

repulsive force given by an external magnet may give rise to a mechanical deformation on the graphene sheet. The detailed study of this is left for a future work.

The authors thank R. S. Ruoff for discussions. This work was supported in part by Grant-in-Aid for Scientific Research on Priority Areas "Carbon Nanotube Nanoelectronics" and by Grant-in-Aid for Scientific Research from Ministry of Education, Culture, Sports, Science and Technology Japan.

-
- [1] J. C. Slonczewski and P. R. Weiss, Phys. Rev. 109, 272 (1958).
 - [2] D. P. DiVincenzo and E. J. Mele, Phys. Rev. B 29, 1685 (1984).
 - [3] G. W. Semenoff, Phys. Rev. Lett. 53, 2449 (1984).
 - [4] T. Ando, J. Phys. Soc. Jpn. 74, 777 (2005) and references cited therein.
 - [5] N. H. Shon and T. Ando, J. Phys. Soc. Jpn. 67, 2421 (1998).
 - [6] Y. Zheng and T. Ando, Phys. Rev. B 65, 245420 (2002).
 - [7] V. P. Gusynin and S. G. Sharapov, Phys. Rev. Lett. 95, 146801 (2005).
 - [8] N. M. R. Peres, F. Guinea, and A. H. Castro Neto, Phys. Rev. B 73, 125411 (2006).
 - [9] K. S. Novoselov et al., Science 306, 666 (2004).
 - [10] K. S. Novoselov et al., Nature 438, 197 (2005).
 - [11] Y. Zhang, Y. W. Tan, H. L. Stormer, and P. Kim, Nature 438, 201 (2005).
 - [12] J. W. McClure, Phys. Rev. 104, 666 (1956).
 - [13] J. W. McClure, Phys. Rev. 119, 606 (1960).
 - [14] M. P. Shamma, L. G. Johnson, and J. W. McClure, Phys. Rev. B 9, 2467 (1974).
 - [15] S. A. Saffran and F. J. DiSalvo, Phys. Rev. B 20, 4889 (1979).
 - [16] J. Blinowski and C. Rigaux, J. Phys. (Paris) 45, 545 (1984).
 - [17] R. Saito and H. Kamimura, Phys. Rev. B 33, 7218 (1986).
 - [18] H. Aji and T. Ando, J. Phys. Soc. Jpn. 62, 2470 (1993); ibid. 63, 4267 (1994); ibid. 64, 4382 (1995).
 - [19] M. Yamamoto, M. Koshino, and T. Ando, J. Phys. Soc. Jpn. 77, 084705 (2008).
 - [20] S. G. Sharapov, V. P. Gusynin, and H. Beck, Phys. Rev. B 69, 075104 (2004).
 - [21] H. Fukuyama, J. Phys. Soc. Jpn. 76, 043711 (2007).
 - [22] M. Koshino and T. Ando, Phys. Rev. B 75, 235333 (2007).
 - [23] M. Koshino and T. Ando, Phys. Rev. B 76, 085425 (2007).
 - [24] M. Nakamura and L. Hirasawa, Phys. Rev. B 77, 045429 (2008).
 - [25] A. H. Castro Neto et al., Rev. Mod. Phys. 81, 109 (2009).
 - [26] A. Ghosal, P. Goswami, and S. Chakravarty, Phys. Rev. B 75, 115123 (2007).
 - [27] N. M. R. Peres, A. H. Castro Neto, and F. Guinea, Phys. Rev. B 73, 241403(R) (2006).
 - [28] A. De Martino, L. Dell'Anna, and R. Egger, Phys. Rev. Lett. 98, 066802 (2007).
 - [29] M. Ramazaniasir, P. Vasileopoulos, A. Matulis, and F.

- M .Peeters, Phys.Rev.B 77, 235443 (2008)
- [30] A .S.Kotosonov, JETP Lett. 43, 37 (1986).
- [31] See, for example, J.M.D .Coey: Rare-earth Iron Permanent Magnets, (Clarendon Press, Oxford, 1996)
- [32] T .Ando, J.Phys.Soc.Jpn., 75, 074716 (2006).
- [33] L.Brey, H .A .Fertig, and S.DasSarma, Phys.Rev.Lett. 99, 116802 (2007).
- [34] P.Esquinazi et al, Phys.Rev.Lett. 91, 227201 (2003).
- [35] Y .Wang et al, Nano Lett. 9, 220 (2009).
- [36] J.Hass et al, Phys.Rev.Lett. 100, 125504 (2008).
- [37] S.Uryu and T .Ando, Phys.Rev.B 72, 245403 (2005).